Dynamics of confined liquids under shear

M. Urbakh,* L. Daikhin, and J. Klafter
School of Chemistry, Tel Aviv University, Tel Aviv 69978, Israel
(Received 6 October 1994)

Shear thinning of confined liquids is studied in the framework of the time-dependent Ginzburg-Landau equation coupled to a shear-induced velocity field. A scaling relationship between the effective viscosity and the shear rate is analytically derived with an exponent that depends on the velocity profile within the liquid and on the boundary conditions. Thinning is observed for shear rates faster than typical liquid relaxation rates. Relevance to existing systems and predictions amenable to new experiments are discussed.

PACS number(s): 68.45.−v, 47.27.Lx, 47.50.+d

I. INTRODUCTION

Understanding the properties of liquids in contact with solid surfaces has been a long standing problem with relevance to a broad range of technological questions as well as to basic issues in theories of interfaces [1,2]. Changes in the nature of liquids at the liquid-solid interface have been observed experimentally and through molecular dynamics calculations. While the peculiarities of the changes in liquid structure near surfaces are quite well documented and understood, much less is known about the dynamical behaviors of liquids under shear [1–4].

In this paper, we concentrate on confined liquids under shear, a problem known as the Couette flow. There has been a revival of interest in this problem, which directly reflects on the fields of tribology and on the general aspects of fluid rheology, following some intriguing experimental results on thin films [3,4]. The latter have stimulated detailed molecular dynamic studies [5–7] and some general theoretical arguments [8]. The main features observed experimentally and through calculations have been (a) structural inhomogeneities induced by the surfaces (layering), (b) substantial increase of the effective viscosity η_{eff} relative to the bulk, and (c) a non-Newtonian behavior that displays a flow-dependent effective viscosity [4]

$$\eta_{\text{eff}} \sim (\dot{\gamma})^{-\alpha} , \tag{1}$$

where $\dot{\gamma}$ is the shear rate, $\dot{\gamma}=V/d$; V being the shear velocity and d the film thickness. The scaling in Eq. (1) corresponds to what is known as shear thinning, namely reduction of the initial effective viscosity with the increase of the shear rate. The reported values of the exponent α have been around $\alpha \cong \frac{2}{3}$, although higher values, $\alpha \cong 1$, have been also observed [4].

Previous studies have focused on molecular dynamics calculations [5–7] and have contributed important microscopic scale information. Here we introduce a theoretical approach to describe the shear-induced properties of confined liquids, which is based on the coupling between the time-dependent Ginzburg-Landau (TDGL) equation for the order parameter $S(\mathbf{r},t)$ and a velocity field [9,10]. The nature of the velocity field can be dictated, as an example, by the Navier-Stokes equation, or can mimic some known behavior related to the structure of the confined liquid. The approach is the extension, to include dynamics, of studies of the Landau-Ginzburg equations for equilibrium properties of confined liquids [10,11]. What we obtain is an analytical derivation of Eq. (1) with an exponent α, which depends on the velocity profile and on the boundary conditions. We emphasize that our approach is not an atomistically realistic description of the system but we rather derive a reasonable continuum description that holds for a large class of systems independent of molecular details.

II. THE MODEL

We consider two walls separated by a liquid film. The planes $z=0$ and $z=d$ are chosen to coincide with the wall surfaces. A flow is generated in the liquid by moving the bottom wall at a constant velocity V in the direction along the axis y. In order to describe the dynamics under shear, we start from the TDGL equation for the local order parameter $S(\mathbf{r},t)$

$$\frac{\partial}{\partial t} S(\mathbf{r},t) = -\Gamma \mu(\mathbf{r},t) - \nabla \cdot [S(\mathbf{r},t)\mathbf{v}(\mathbf{r},t)] , \tag{2}$$

where Γ is the kinetic coefficient, which describes the relaxation of the order parameter, $\mathbf{v}(\mathbf{r},t)$ is the local velocity, and $\mu(\mathbf{r},t)$ is the local chemical potential, which is expressed as

$$\mu(\mathbf{r},t) = \frac{\delta H\{S\}}{\delta S(\mathbf{r},t)} . \tag{3}$$

Here $H\{S\}$ is the Ginzburg-Landau type free-energy functional

*Electronic address: urbakh@ccsg.tau.ac.il

$$H\{S\}=\int d\mathbf{r}\left[\frac{a}{2}[\nabla S(\mathbf{r},t)]^2+\frac{\tau}{2}S(\mathbf{r},t)^2+\cdots\right], \quad (4)$$

where a and τ are positive coefficients. As we aim at a general continuum description, the order parameter may mimic liquid density, polarization of liquid molecules, their orientation, local number of near neighbors, etc. The effect of the substrate on the liquid structure is introduced by adding surface terms to the free energy of the system

$$H_s\{S\}=\sum_{i=1,2}\int d\mathbf{r}\,\delta(z-z)_i[-h_i(\mathbf{R}-\delta_{i,1}\mathbf{V}t)S(\mathbf{r},t)+\tfrac{1}{2}C_iS^2(\mathbf{r},t)+\cdots], \quad (5)$$

where $z_1=0$ and $z_2=d$ and $\mathbf{R}=(x,y)$. A similar model, with uniform interactions h_i along the interfaces has been used to study wetting phenomena [12]. The free-energy functional in Eq. (5) introduces the preferred value of the order parameter at the surface, $S(z=z_i,\mathbf{R})=h_i(\mathbf{R})/C_i$, $i=1,2$. The values of the parameters h_i/a and C_i/a determine the equilibrium state at the interface [12]. Here we take into account the lateral nonuniformity of the liquid-solid interactions, which plays an essential role in the dynamics of confined liquids. The importance of this new aspect has been emphasized in recent molecular dynamic calculations [5–7]. As an example, we assume periodically varying liquid-substrate interactions along the interfaces, $h_i(\mathbf{R})=h\sin(2\pi y/l)$.

The calculations have been done for the quadratic form of the free-energy, Eq. (4), which is simple to handle but yet rich enough to lead to shear-induced effects. In this case, the parameters $(a/\tau)^{1/2}$ and $1/(\Gamma\tau)$ are the correlation length and relaxation time in the liquid.

The boundary conditions for the order parameter $S(\mathbf{r},t)$ at the two walls, the movable and fixed follow from the Eqs. (4) and (5) for the free energy and are

$$a\frac{\partial}{\partial z}S(z=0,\mathbf{R},t)=C_1S(z=0,\mathbf{R},t)-h_1(\mathbf{R}-\mathbf{V}t), \quad (6)$$

$$a\frac{\partial}{\partial z}S(z=d,\mathbf{R},t)=-C_2S(z=d,\mathbf{R},t)+h_2(\mathbf{R}). \quad (7)$$

In order to study the dynamics of the order parameter, one needs the velocity distribution in the liquid film. We assume that the liquid is incompressible and that the velocity obeys the modified Navier-Stokes equation, with viscosity η, which includes the force associated with a local stress created by the inhomogeneous order parameter [9]. For the velocities within the liquid, we use the stick boundary conditions. It should be emphasized that considering the Navier-Stokes equation should be viewed only as an example of how velocities can be coupled to the liquid order parameter (although molecular dynamic studies in thin films [5], which show that $\eta_{\text{eff}}\neq$const, still exhibit a Navier-Stokes-like behavior of the velocity field). The approach is more general, as will be shortly shown, and different velocity distributions can be deduced from other equations relevant to the problem.

The frictional force per unit area, $\mathbf{F}$, which is the experimental observable, can be found from the energy balance in the system. Equation (2) for the order parameter and the Navier-Stokes equation lead to the following expression for the frictional force

$$\mathbf{F}=\frac{1}{V\mathbf{L}^2}\left\{\eta\int d\mathbf{R}[\mathbf{v}(\nabla\mathbf{v})+(\mathbf{v}\nabla)\mathbf{v}]\Big|_{z=0}-a\int d\mathbf{R}\left[\frac{\partial}{\partial z}S(z=0,\mathbf{R},t)\right]\frac{\partial}{\partial t}S(z=0,\mathbf{R},t)\right\}, \quad (8)$$

where $\mathbf{L}^2$ is the surface area. The first term in Eq. (8) describes the usual viscous friction at the solid-liquid interface and the second term gives an additional contribution associated to the dynamics of ordering in the liquid film. Below we focus on the latter contribution, which depends strongly on the liquid-substrate interaction and on the thickness of the film. The effective viscosity of the sheared liquid film η_{eff} is defined [3,4] as $\eta_{\text{eff}}=Fd/V$. Experimentally it has been observed that η_{eff} of confined liquids is usually $\sim 10^4\eta$, which means that the second term in Eq. (8), on which we concentrate, dominates. The main effect here is a boundary effect, which induces some structure in the confined liquid represented by the order parameter. In the limit of $d\to\infty$, where there is no boundary effect, one recovers the bulk behavior, in which only the first term in Eq. (8) contributes and the order parameter is zero.

Equation (2) has to be solved self-consistently with the equation for the velocity field. In the case of zero force, associated with the order parameter, the solution of Navier-Stokes equation with no-slip boundary conditions gives a linear velocity distribution in the film. Both molecular dynamics simulations [5–7] and perturbation theory with respect to that force [13] show that flow near solid boundaries depends on the strength of the wall-liquid interaction. For strong interactions, of interest in the present paper, the liquid layers adjacent to the two interfaces may be partially locked to the solid walls and the velocity profile is close to linear between these layers [5–7].

We do not solve the problem self-consistently, but instead present the results of an approximate solution for two limiting velocity distributions. Based on the considerations given above, we have chosen the following two distributions: (1) a linear one that is reasonable for thick enough "liquidlike" films and (2) a step-wise distribution ($\mathbf{v}=\mathbf{V}$ for $z\le d/2$ and $\mathbf{v}=\mathbf{0}$ for $z>d/2$), which simulates velocity profile in thin "solidlike" films. In both cases the problem is solved analytically. For this purpose, it is convenient to Fourier transform the order parameter $S(\mathbf{r},t)\to S(\mathbf{z},\mathbf{K},\omega)$. The solutions are expressed in terms of two dimensionless parameters

$$u=d/l_{\text{eff}} \quad \text{and} \quad g=\omega(\tau\Gamma)^{-1}\frac{l_{\text{eff}}^2}{a/\tau}, \quad (9)$$

where $l_{\text{eff}}=[(\tau/a)+K^2]^{-1/2}$ is the effective length that characterizes the lateral nonuniformity of the liquid film caused by the "bulk" fluctuations of the order parameter and by nonuniformity of the liquid-substrate interactions.

In contrast to the equilibrium properties that are determined mostly by the vertical nonuniformity of liquid films [11], the energy dissipation in our dynamical system is affected by the lateral nonuniformity. For the particular sinusoidal choice mentioned above, with period l, of the liquid-solid interaction one obtains $K=2\pi/l$ and $\omega=-(\mathbf{K}\cdot\mathbf{V})$. The parameter u is the ratio of the transversal length d and the lateral length l_{eff} and the parameter g is proportional to the ratio of the liquid relaxation time $(\Gamma\tau)^{-1}$ and the characteristic time of the wall motion l/V. The parameter g in Eq. (9) is proportional to the shear rate $\dot\gamma$ and can be rewritten as $g=\dot\gamma/\dot\gamma_0$ where $\dot\gamma_0=al\Gamma/(2\pi dl_{\text{eff}}^2)$ and characterizes the relaxation rate in the liquid. Within our model, the rate $\dot\gamma_0$ is related to relaxation of some lateral structure.

Linear velocity distribution (liquidlike film)

The solution of the dynamic equation for the Fourier component of the order parameter is expressed in terms of Airy functions and leads to the following asymptotic behavior for the effective viscosity at low and high shear rates (see Appendix A)

$$\eta_{\text{eff}}=\frac{\pi^2\mathbf{h}^2dl_{\text{eff}}^3}{a^2l^2\Gamma}\times\begin{cases}\frac{1}{2}u^{-1}(\delta+1)^{-2} & \text{at } \dot\gamma/\dot\gamma_0\ll 1\\ \dfrac{2\pi}{(u\sqrt{3})^{1/3}\Gamma(\frac{1}{3})^2}\left[\dfrac{\dot\gamma}{\dot\gamma_0}\right]^{-2/3}\left|\delta-\dfrac{\pi(1+i/\sqrt{3})}{\Gamma(\frac{1}{3})^2}\left[\dfrac{3\dot\gamma}{u\dot\gamma_0}\right]^{1/3}\right|^{-2} & \text{at } \dot\gamma/\dot\gamma_0\gg 1\ .\end{cases}\tag{10}$$

Equation (10) demonstrates that the viscosity reaches its maximum value at low shear rates and remains almost constant in this region ($\dot\gamma/\dot\gamma_0\ll 1$); in the high shear rate limit ($\dot\gamma/\dot\gamma_0>1$) the viscosity exhibits shear thinning according to Eq. (1) with a characteristic exponent, α, which depends on the parameter $\delta=Cl_{\text{eff}}/a$. For $\delta\ll 1$, we obtain $\alpha=\frac{4}{3}$ while for $\delta>1$ we obtain in the region of intermediate asymptotics ($1\le\dot\gamma/\dot\gamma_0<u\delta^3$) $\alpha=\frac{2}{3}$ as observed in experiments and in molecular dynamics simulations [4,5]. It should be pointed out that our calculations assume a constant film thickness, while the $\frac{2}{3}$ power law observed in experiments and simulations corresponds to the condition of constant normal pressure. However, the experiments were unable to detect a variation of the layer thickness with shear rate and similar results for the exponent were obtained in simulations for the constant thickness [4,5]. The dependence of the effective viscosity on the shear rate calculated over a broad range of $\dot\gamma$ values for different values of the parameter δ is shown in Fig. 1. Our calculations also show that the effective viscosity of the liquidlike films only slightly depends on the thickness d, demonstrating power-law dependence.

Step-wise velocity distribution (solidlike film)

For the step-wise velocity profile, which represents two locked regions, we arrive at the following asymptotic behavior:

$$\eta_{\text{eff}}=\frac{\pi^2h^2dl_{\text{eff}}^3}{a^2l^2\Gamma}(\delta+l)^{-2}e^{-u}\times\begin{cases}1 & \text{at } \dot\gamma/\dot\gamma_0\ll 1\\ 4\sqrt{2}(\dot\gamma/\dot\gamma_0)^{-3/2} & \text{at } \dot\gamma/\dot\gamma_0\gg 1\ .\end{cases}\tag{11}$$

As before, the viscosity reaches its maximum value at low shear rates and exhibits shear thinning in the high shear rate limit. In contrast to the liquidlike films, the characteristic exponent here is $\alpha=\frac{3}{2}$ and is independent of the parameter δ. The dependence of the effective viscosity on the shear rate for the solidlike films is presented in Fig. 2.

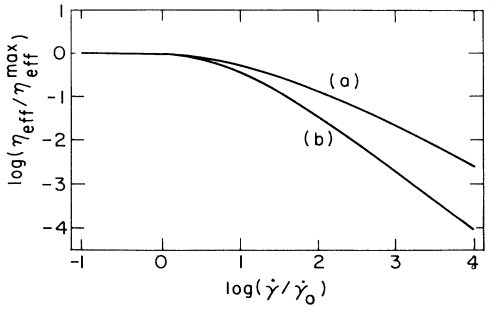

FIG. 1. Log_{10}-log_{10} representation of the reduced effective viscosity as a function of the reduced shear rate obtained for liquidlike films with the thickness $d=4l_{\text{eff}}$ and (a) $\delta=10$, for which $\alpha=\frac{2}{3}$, and (b) $\delta=0.1$, for which $\alpha=\frac{4}{3}$.

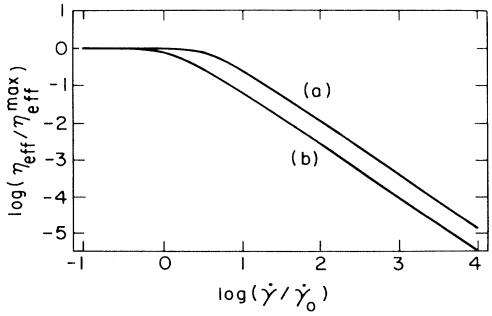

FIG. 2. Log_{10}-log_{10} representation of the reduced effective viscosity as a function of the reduced shear rate obtained for solidlike films with the thickness $d=2l_{\text{eff}}$ and (a) $\delta=10$ and (b) $\delta=0.1$. In both cases $\alpha=\frac{3}{2}$.

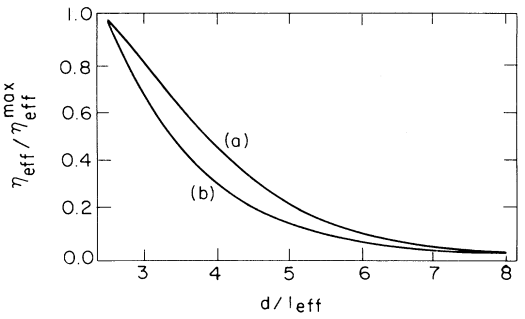

FIG. 3. Variation of the reduced effective viscosity of solidlike films with the reduced thickness at low shear rates for (a) $\delta=10$ and (b) $\delta=0.1$.

Equation (11) is characterized by an exponential dependence of the effective viscosity of a solidlike film on its thickness (see Fig. 3). We note that the step-wise velocity distribution may be appropriate for the description of ultrathin surface layers in which the molecules are chemically attached to the surfaces, a case that has been recently studied experimentally [14]. In this case, we have a definite plane of slippage as assumed in the model discussed above. Experimental studies indicate that under high pressures ultrathin layers of liquids also show solidlike behavior [14].

III. DISCUSSION

The results in Eqs. (10) and (11) demonstrate that shear thinning is a quite general phenomenon and does not depend on the details of intermolecular interactions in the liquid and between the liquid and the substrate. The non-Newtonian behavior arises when the relaxation time of the liquid structure induced by the interaction with the laterally nonuniform interfaces becomes larger than the time at which the wall passes the length characterizing the lateral ordering, namely $g=\dot{\gamma}/\dot{\gamma}_0>1$. The value of the exponent α, the maximum value of the effective viscosity, and the magnitude of critical shear rate $\dot{\gamma}_c$ at which the non-Newtonian behavior starts, depend on the properties of the system: the film thickness, the boundary conditions on the order parameter, and the velocity distribution in the liquid film. Our calculations show that the exponent α spans the interval $\frac{2}{3}\leq\alpha\leq\frac{3}{2}$. The exponent reaches the lower and upper bound values in the two limiting cases, respectively, the liquidlike films with the linear velocity distribution and the solidlike films with the step-wise velocity distribution. For intermediate velocity distributions, which we do not discuss in detail here, we expect the exponent α to lie between $\frac{2}{3}$ and $\frac{3}{2}$. It should be stressed that the exponents discussed above describe the asymptotic behavior of the effective viscosity for high shear rates. The values found from the experimental data could be smaller if the asymptotic region is not reached during the measurements. The predicted values of the exponent α depend on the velocity profiles, which should be obtained in a self-consistent way from Eq. (2) and the Navier-Stokes equation. The velocity profile itself may change with the shear rate. Here we presented only the approximate solution of the equations, which holds for the given velocity profiles. The self-consistent solution may still change the values of the exponent.

The experimental observation [4] of a strong dependence of $\eta_{\rm eff}$ on thickness for very thin films can be explained under the assumption that the step-wise velocity distribution is applicable. With the increase of the thickness, the velocity distribution changes to the linear profile and the film passes from the solidlike to the liquidlike state. As a result, the effective viscosity loses its pronounced dependence on the film thickness, as observed experimentally [4]. It should be mentioned that within our model this transition is not related to any phase transition in the system. The observation of the exponent $\alpha\approx\frac{2}{3}$ may indicate that the film is close to the liquidlike state and that $\delta>1$ [see Eq. (10)]. It is important to note that this value of the exponent has been obtained in the region of the thicknesses where the effective viscosity only slightly depends on the thickness that gives additional support to the above statement.

In conclusion, shear thinning is obtained in the framework of the TDLG equation coupled to a velocity field for shear rates faster than relaxation rates in the liquid. The scaling relationship, Eq. (1), emerges naturally from the model with a scaling exponent which depends on the nature of the velocity field and on the boundary conditions. Our results demonstrate that the thinning is enhanced in the step-wise velocity case ($\alpha=\frac{3}{2}$) relative to the hydrodynamic, liquidlike case ($\alpha=\frac{4}{3}$ or $\alpha=\frac{2}{3}$). In the liquidlike regime a dependence on surface wetting is predicted, which should be amenable to experimental observation by changing the liquid-wall interactions. The experimental findings of thinning with $\alpha\approx\frac{2}{3}$ and the dependence $\eta_{\rm eff}$ on liquid thickness concur with a possible solidlike to liquidlike transition.

ACKNOWLEDGMENT

Financial support for this work by the Israel Science Foundation administered by the Israel Academy of Science and Humanities is gratefully acknowledged.

APPENDIX

For the linear velocity distribution $\mathbf{v}(z)=\mathbf{V}(1-z/d)$, the dynamic Eq. (2) takes the following form in the $(z,\mathbf{K},\omega)$ representation:

$$\left[\frac{\partial^2}{\partial z^2}-\left[\frac{\tau}{a}+\mathbf{K}^2+\frac{i\omega}{a\Gamma}\right]-\frac{i(\mathbf{K}\cdot\mathbf{V})}{a\Gamma}(1-z/d)\right]\times S(z,\mathbf{K},\omega)=0\ . \quad \text{(A1)}$$

The boundary conditions (6) and (7) transform to

$$a\frac{\partial}{\partial z}S(z=0,\mathbf{K},\omega)=C_1S(z=0,\mathbf{K},\omega)-2\pi h_1(\mathbf{K})\delta[\omega+(\mathbf{K}\cdot\mathbf{V})]\ , \quad \text{(A2)}$$

$$a\frac{\partial}{\partial z}S(z=d,\mathbf{K},\omega)=-C_2S(z=d,\mathbf{K},\omega)=2\pi h_2(\mathbf{K})\delta(\omega)\ . \tag{A3}$$

For the particular form of the liquid-substrate interaction $h_i(\mathbf{R})=h\sin(2\pi y/l)$ considered here, the wave vector $\mathbf{K}$ takes the value $\mathbf{K}=(0,\pm 2\pi/l)$.

The solution of Eq. (A1) is expressed through the Airy functions [15]

$$S(z,\mathbf{K},\omega)=D_1\mathrm{Ai}(\xi)+D_2\mathrm{Bi}(\xi)\ , \tag{A4}$$

where

$$\xi=-(igu^2)^{1/3}\left[\frac{z}{d}+ig^{-1}\right]\ . \tag{A5}$$

The prefactors D_1 and D_2 are obtained from the boundary conditions (A2) and (A3):

$$D_1=2\pi A_{11}(\mathbf{K})h_1(\mathbf{K})\delta[\omega+(\mathbf{K}\cdot\mathbf{V})] -2\pi A_{12}(\mathbf{K})h_2(\mathbf{K})\delta(\omega)\ , \tag{A6}$$

$$D_2=2\pi A_{21}(\mathbf{K})h_1(\mathbf{K})\delta[\omega+(\mathbf{K}\cdot\mathbf{V})] +2\pi A_{22}(\mathbf{K})h_2(\mathbf{K})\delta(\omega)\ . \tag{A7}$$

Here

$$\begin{aligned}
&A_{11}(\mathbf{K})=[-\kappa\,\mathrm{Bi}'(\xi_2)+C_2\mathrm{Bi}(\xi_2)]/Dt\ ,\quad A_{12}(\mathbf{K})]=[\kappa\,\mathrm{Bi}'(\xi_1)+C_1\mathrm{Bi}(\xi_1)]/Dt\ ,\\
&A_{21}(\mathbf{K})=[\kappa\,\mathrm{Ai}'(\xi_2)-C_2\mathrm{Bi}(\xi_2)]/Dt\ ,\quad A_{22}(\mathbf{K})=[\kappa\,\mathrm{Ai}'(\xi_1)+C_1\mathrm{Ai}(\xi_1)]/Dt\\
&\kappa=[i(\mathbf{K}\cdot\mathbf{V})/(a\Gamma d)]^{1/3}\ ,\quad \xi_1=\xi(z=0)=(i^{-1}g^{-1}u)^{2/3}\ ,\quad \xi_2=\xi(z=d)=-(igu^2)^{1/3}[1+ig^{-1}]\ ,\\
&Dt=[\kappa\,\mathrm{Ai}'(\xi_1)+C_1\mathrm{Ai}(\xi_1)][-\kappa\,\mathrm{Bi}'(\xi_2)+C_2\mathrm{Bi}(\xi_2)]-[-\kappa\,\mathrm{Ai}'(\xi_2)+C_2\mathrm{Ai}(\xi_2)][\kappa\,\mathrm{Bi}'(\xi_1)+C_1\mathrm{Bi}(\xi_1)]
\end{aligned} \tag{A8}$$

and prime denotes the derivative with respect to ξ.

Substitution of Eqs. (A4), (A6), and (A7) into Eq. (8) leads to the following expression for the frictional force

$$\begin{aligned}
F=-\frac{a\pi h^2}{l}\mathrm{Im}\{\kappa[\,|A_{11}(2\pi/l)|^2\mathrm{Ai}'(\xi_1)\mathrm{Ai}^*(\xi_1)+|A_{21}(2\pi/l)|^2\mathrm{Bi}'(\xi_1)\mathrm{Bi}^*(\xi_1)\\
+A_{11}^*(2\pi/l)A_{21}(2\pi/l)\mathrm{Bi}'(\xi_1)\mathrm{Ai}^*(\xi_1)+A_{11}(2\pi/l)A_{21}^*(2\pi/l)\mathrm{Ai}'(\xi_1)\mathrm{Bi}^*(\xi_1)]\}\ .
\end{aligned} \tag{A9}$$

Using the asymptotic expressions for the Airy functions [15] in Eq. (A9), we arrive at Eq. (10) for the effective viscosity.

Similar calculations have been carried out for the step-wise velocity distribution.

[1] *Fundamentals of Friction,* edited by I. L. Singer and H. M. Pollock (Kluwer, Dordrecht, 1992).

[2] MRS Bull. **18**, (5), (1993).

[3] M. L. Gee, P. M. McGuiggan, and J. N. Israelachvili, J. Chem. Phys. **93**, 1895 (1990); H. Yoshizawa, P. M. McGuiggan, and J. N. Israelachvili, Science **259**, 1305 (1993).

[4] J. Van Alsten and S. Granick, Phys. Rev. Lett. **61**, 2570 (1988); H.-W. Hu, G. A. Carson, and S. Granick, Phys. Rev. Lett. **66**, 2758 (1991); S. Granick, Science **253**, 1374 (1992).

[5] P. A. Thompson and M. O. Robbins, Phys. Rev. A **41**, 6830 (1990); Science **250**, 792 (1990); P. A. Thompson, G. S. Grest, and M. O. Robbins, Phys. Rev. Lett. **66**, 3448 (1992).

[6] I. Bitsanis, J. J. Magda, H. T. Davis, and M. Tirrell, J. Chem. Phys. **87**, 1733 (1987); I. Bitsanis, S. A. Somers, H. T. Davis, and M. Tirrell, *ibid.* **93**, 3427 (1990).

[7] L. Bocquet and J.-L. Barrat, Phys. Rev. Lett. **70**, 2726 (1993); Phys. Rev. B **49**, 3079 (1994).

[8] Y. Rabin and I. Hersht, Physica A **200**, 708 (1993).

[9] K. Kawasaki, Ann. Phys. (N.Y.) **61**, 1 (1970); T. Koga and K. Kawasaki, Physica A **196**, 389 (1993); T. Koga, K. Kawasaki, M. Takenaka, and T. Hashimoto, Physica A **198**, 473 (1993).

[10] P. C. Hohenberg and B. I. Halperin, Rev. Mod. Phys. **49**, 435 (1977).

[11] S. Marcelja and N. Radic, Chem. Phys. Lett. **42**, 129 (1976); M. E. Fisher and H. Nakanishi, J. Chem. Phys. **75**, 5857 (1981); R. Evans, J. Phys. Condens. Matter **2**, 8989 (1990); S. Dietrich, in *Phase Transitions and Critical Phenomena,* edited by C. Domb and J. L. Lebowitz (Academic, New York, 1988), Vol. 12, p. 1.

[12] P. G. de Gennes, Rev. Mod. Phys. **57**, 827 (1985).

[13] The results of the solution of the Navier-Stokes equation within the perturbative approach will be presented in a future presentation.

[14] G. Reiter, A. L. Demirel, J. Peanasky, L. L. Cai, and S. Granick, J. Chem. Phys. **101**, 2606 (1994).

[15] *Handbook of Mathematical Functions,* edited by M. Abramowitz and I. Stegun (Dover, New York, 1965).